Vol. 2 No. 3 JOURNAL OF COMPUTATIONAL MATHEMATICS July 1984

NUMERICAL COMPUTATION OF FLOW FIELD WITH DEFLAGRATION AND DETONATION*[1)]

WU XIONG-HUA (吴雄华) WANG YONG (王 勇)

(Computing Center, Academia Sinica, Beijing, China)

TENG ZHEN-HUAN (滕振寰)

(Peking University, Beijing, China)

ZHU YOU-LAN (朱幼兰)

(Computing Center, Academia Sinica, Beijing, China)

I. Introduction

The problems involving combustion are increasingly important, and are attracting more and more attention. The task for the computational mathematicians is to compute accurately the flow fields with combustion waves. The transition from deflagration to detonation is an important problem in the combustion phenomenon. Because the velocity and the strength of detonation are much larger than those of deflagration, detonation is much more dangerous than deflagration. [1] has computed the flow fields generated by accelerated flames using the floating-shock-fitting method. [2] has also computed such problems using the random choice method and showed how to determine the transition from deflagration to detonation by numerical methods. In this paper the singularity-separating method (S. S. M. for short) is used to compute the whole flow fields with transition to detonation. The comparison between the results of the random choice method (R. C. M. for short) and our method is presented. Because there are many complicated interactions between different discontinuity lines, such a combustion problem is a good choice for testing numerical methods. The solution obtained by S. S. M. has the second order accuracy not only in the smooth regions but also in the regions near the discontinuity lines.

II. Formulation of the Problem

The system of nonlinear gas dynamics is

$$\begin{cases} \dfrac{\partial u}{\partial t}+u\dfrac{\partial u}{\partial x}+\dfrac{1}{\rho}\dfrac{\partial p}{\partial x}=0, \\ \dfrac{\partial \rho}{\partial t}+u\dfrac{\partial \rho}{\partial x}+\rho\dfrac{\partial u}{\partial x}=0, \\ \dfrac{\partial p}{\partial t}+u\dfrac{\partial p}{\partial x}+\gamma p\dfrac{\partial u}{\partial x}=0. \end{cases} \tag{1}$$

* Received November 29, 1983.

1) This work was supported by the Science Foundation of Academia Sinica under M-82-392.

Throughout this paper, the subscript 1 refers to burned gas and the subscript 0 unburned gas, V stands for the velocity of the reacting front, Q for the energy released by unit gas in the process of reaction, γ for ratio of specific heats, ρ, u, p and c for the density, gas velocity, pressure and sound velocity respectively. The relations of combustion wave in the polytropic gas are

$$\rho_0(u_0-V)=\rho_1(u_1-V), \tag{2}$$

$$\rho_0(u_0-V)^2+p_0=\rho_1(u_1-V)^2+p_1, \tag{3}$$

$$\frac{1}{\gamma_0-1}\frac{p_0}{\rho_0}-\frac{1}{\gamma_1-1}\frac{p_1}{\rho_1}+Q=\frac{1}{2}\left(\frac{1}{\rho_0}-\frac{1}{\rho_1}\right)(p_0+p_1). \tag{4}$$

From the above formulae the following formulae for the strong detonation, the C–J detonation and the weak deflagration can be obtained. The relations of the strong detonation are

$$V=\frac{\rho_1u_1-\rho_0u_0}{\rho_1-\rho_0}, \tag{5}$$

$$\rho_1=\rho_0\frac{\dfrac{\gamma_1+1}{\gamma_1-1}\dfrac{p_1}{p_0}+1}{\dfrac{\gamma_0+1}{\gamma_0-1}+\dfrac{p_1}{p_0}+2Q\dfrac{\rho_0}{p_0}}, \tag{6}$$

and

$$u_1=u_0\pm\psi(p_1;\ p_0,\ \rho_0). \tag{7}$$

Here, the upper sign stands for the first family of waves and the lower sign for the second family, and

$$\psi(p_1;\ p_0,\ \rho_0)=\sqrt{\frac{(p_1-p_0)\left(\dfrac{2}{\gamma_1-1}p_1-\dfrac{2}{\gamma_0-1}p_0-2\rho_0Q\right)}{\rho_0\left(\dfrac{\gamma_1+1}{\gamma_1-1}p_1+p_0\right)}}. \tag{8}$$

The relations of the C–J detonation are

$$M_0^*=\pm\left(\sqrt{\frac{\gamma_1-1}{2}\left[(\gamma_1+1)\frac{Q}{c_0^2}+\frac{\gamma_1+\gamma_0}{\gamma_0(\gamma_0-1)}\right]}+\sqrt{\frac{\gamma_1+1}{2}\left[(\gamma_1-1)\frac{Q}{c_0^2}-\frac{\gamma_0-\gamma_1}{\gamma_0(\gamma_0-1)}\right]}\right), \tag{9}$$

$$p_J=p_0+p_0\frac{\gamma_0}{\gamma_1+1}\left(M_0^{*2}-\frac{\gamma_1}{\gamma_0}\right), \tag{10}$$

$$u_J=u_0+c_0\frac{1}{\gamma_1+1}\left(M_0^*-\frac{\gamma}{\gamma_0M_0^*}\right), \tag{11}$$

$$\rho_J=\rho_0\Big/\left(1-\frac{1}{\gamma_1+1}\left(1-\frac{\gamma_1}{\gamma_0M_0^{*2}}\right)\right). \tag{12}$$

Because there are two characteristic lines entering a weak deflagration front in one side and only one in the other side, there must be one more condition for determining a weak deflagration. The following formula for the velocity of weak deflagration is used in our computation (see [2])

$$V=u_0+K\left(\frac{p_0}{\rho_0}\right)^{\hat{Q}}, \tag{13}$$

where the constants K and $\hat{Q}$ are determined by experiments. Suppose that

$$M_0=\frac{K}{\sqrt{\gamma_0}}\left(\frac{p_0}{\rho_0}\right)^{\hat{Q}-\frac{1}{2}}. \tag{14}$$

The relations of weak deflagration are

$$p_1=p_0\left(\frac{1+\gamma_0 M_0^2}{\gamma_1+1}+\sqrt{\left(\frac{\gamma_1-\gamma_0 M_0^2}{\gamma_1+1}\right)^2+\frac{2\gamma_0 M_0^2}{T_0(\gamma_1+1)}\left(\frac{(\gamma_0-\gamma_1)c_0^2}{\gamma_0-1}-(\gamma_0-1)Q\right)}\right), \tag{15}$$

$$u_1=u_0\mp\psi(p_1;\ p_0,\ \rho_0), \tag{16}$$

the formula for ψ is the same as (8) and the formula for ρ_1 is the same as (6).

Take the first family of combustion waves as an example. The solution of the Riemann problem of combustion gas is illustrated in Figs. 1—3.

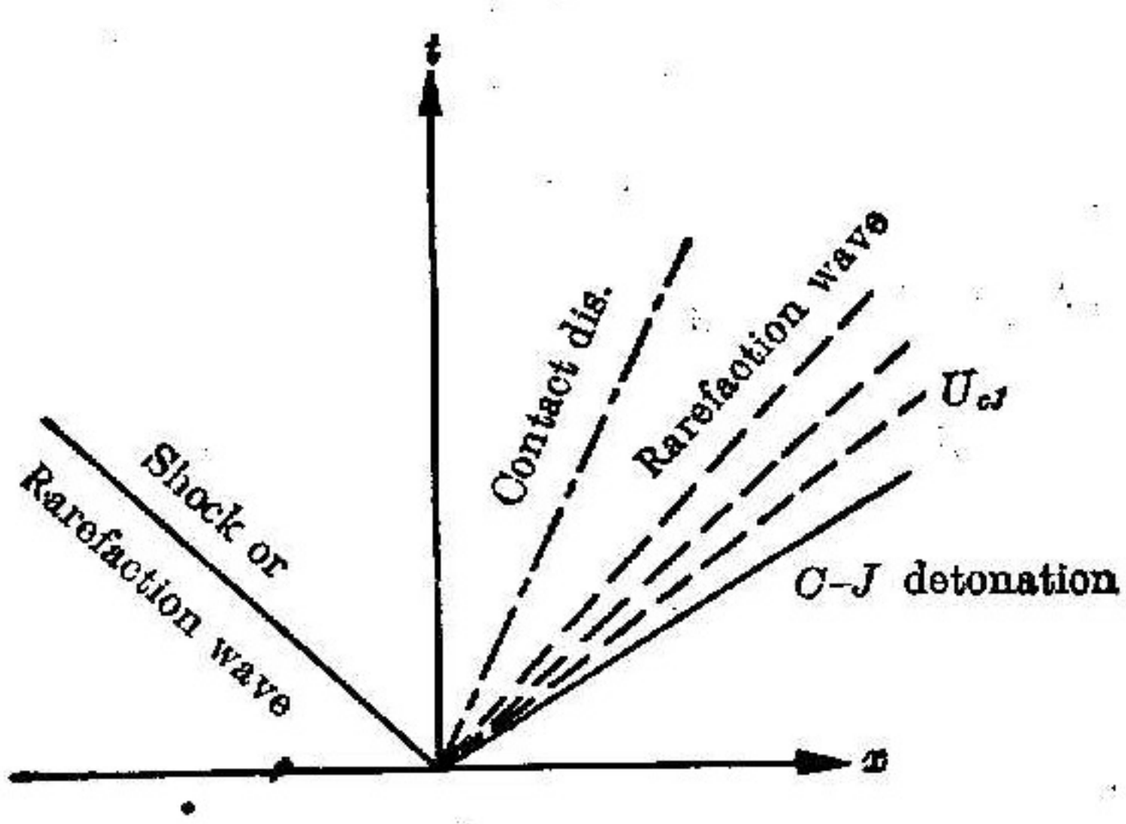

Fig. 1 A Riemann solution with a right C–J detonation

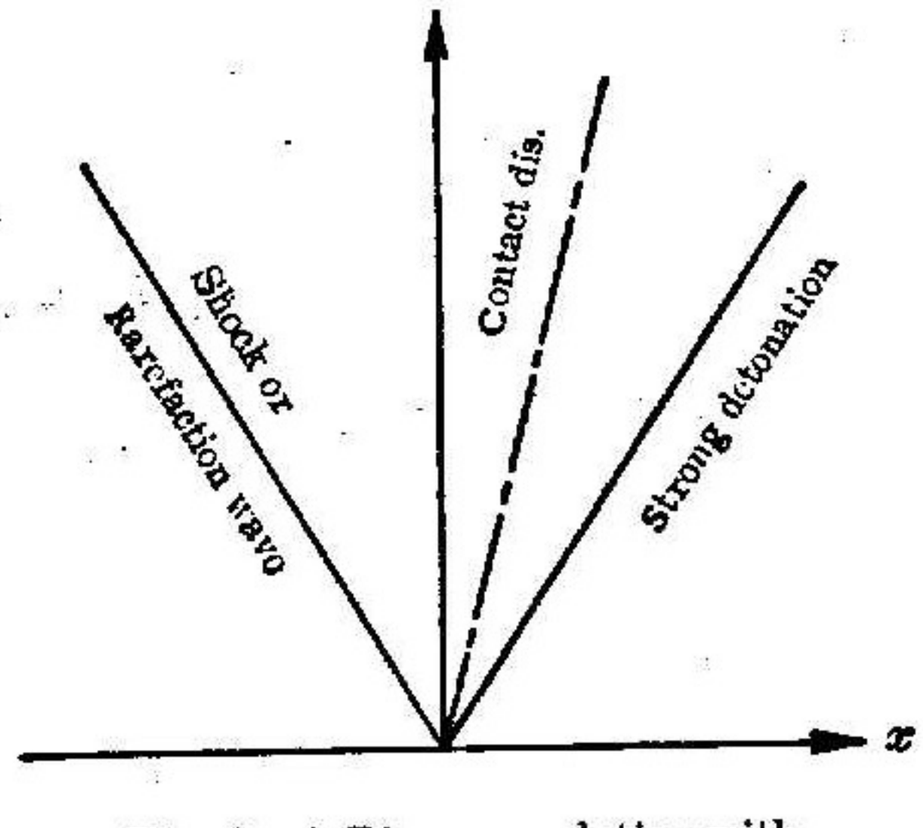

Fig. 2 A Riemann solution with a strong detonation

The solution with a C–J detonation is shown in Fig. 1. There are a shock or a rarefaction wave on the left side, a contact discontinuity in the middle and a C–J detonation followed by a rarefaction wave on the right side. The solution with a strong detonation is shown in Fig. 2. The solution with a weak deflagration is shown in Fig. 3. The condition for the transition from deflagration to detonation used here is the same as in [2], that is, if there is no solution for the Riemann problem with a weak deflagration, a transition happens, and we must solve the Riemann problem with a strong detonation instead.

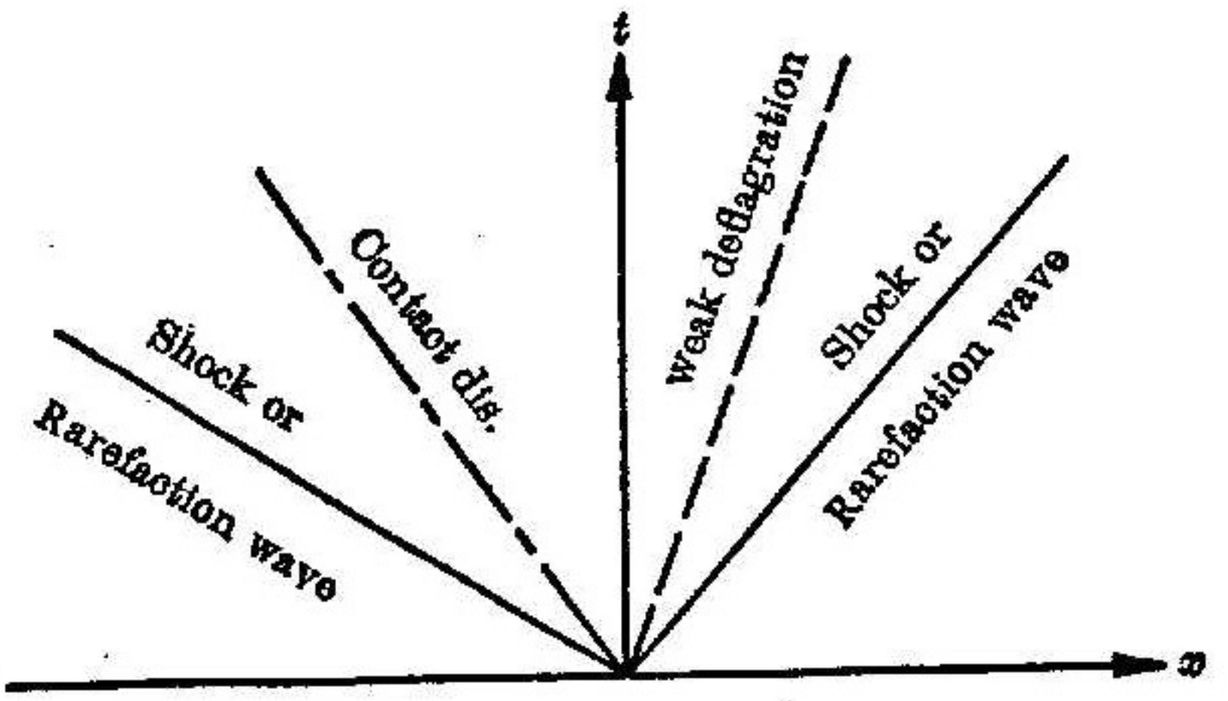

Fig. 3 A Riemann solution with a deflagration wave

In this paper S. S. M. is used for computation of the two examples in [2], the ignition problem and the accelerated flame problem. Not only are the problems with the same medium solved but also those with different media.

Assume the reaction takes place in a tube with a closed end. Let the origin 0 be the closed end, and the positive x–axis be along the tube. The state of gas at rest is $\rho(x,\ 0)=1$, $p(x,\ 0)=1$, $u(x,\ 0)=0$, $x>0$.

1) The ignition problem can be described as follows. Assume that $Q=20$, $\hat{Q}=2$, and the gas is ignited at $x=8$. A right-facing deflagration and a left-facing

deflagration are produced and there is a shock wave before each deflagration. After the left-facing shock is reflected from the closed end, the reflected shock wave interacts with two combustion waves successively. When the reflected shock first hits the right deflagration, the transition from the deflagration to the detonation occurs. The following two cases are computed:

① $\gamma_1=\gamma_0=1.4$, $K=0.1$, and ② $\gamma_1=1.35$, $\gamma_0=1.4$, $K=0.105$.

2) The accelerated flame problem can be described as follows. The gas is ignited at $x=0$. When the flame propagates to $x=5$, its speed coefficient K is suddenly increased by a finite increment ΔK. The parameters are $\hat{Q}=2.6$, $\gamma_1=\gamma_0=1.26$, $Q=27$, $K=0.03367$ and $\Delta K=0.08667$. The transition does not happen immediately after a shock hits the deflagration, but a little later when the deflagration meets a contact discontinuity line.

III. Numerical Methods

The main idea of S. S. M. is the following:

1) Use the coordinate transformation

$$\xi=\frac{x-x_i(t)}{x_{i+1}(t)-x_i(t)}+i, \quad t=t \tag{17}$$

to transform an arbitrary subregion, with boundaries are $x_i(t)$ and $x_{i+1}(t)$ into a strip whose boundaries are $\xi=i$ and $\xi=i+1$ on the ξ–t plane. Such a transformation makes it easy to establish the difference scheme in each rectangular region.

2) Establish the difference scheme in each subregion. Let the differential equation be

$$G\frac{\partial U}{\partial t}+\lambda G\frac{\partial U}{\partial \xi}=0. \tag{18}$$

(Here, U is a vector whose components are u, ρ, p. The system of equations (1) can be transformed into three equations with a form of (18) by multiplying it from the left hand by a transformation matrix.) In what follows we use the notation $\sigma=\lambda\frac{\Delta t}{\Delta\xi}$, where λ is the characteristic value in (18). If $|\sigma|\leqslant 1$, we take the explicit scheme:

At the auxiliary level the formula is

$$G_m^k U_m^{k\pm 1/2}=(1\mp\sigma_m^k/2)G_m^k U_m^k\pm\sigma_m^k G_m^k U_{m\mp 1}^k/2,$$

where we take the upper sign if $\sigma>0$ or the lower sign if $\sigma<0$. At the regular level the formula is

$$[(1-B_m)(G_{m+1}^{k+1/2}+G_m^{k+1/2})+B_m(G_m^{k+1/2}+G_{m-1}^{k+1/2})]U_m^{k+1}=(1-B_m)S_m^1+B_m S_m^2,$$

where B_m is such a number that it is zero on the left boundary, and one on the right boundary, and the variation of B_m is smooth, and

$$\begin{aligned}S_m^1=&(G_m^{k+1/2}+G_{m+1}^{k+1/2})U_{m+1}^k-[(\sigma_{m+1}^{k+1/2}+\sigma_m^{k+1/2})/2+1]\\&\times(G_m^{k+1/2}+G_{m+1}^{k+1/2})(U_{m+1}^{k+1/2}-U_m^{k+1/2}),\\S_m^2=&(G_{m-1}^{k+1/2}+G_m^{k+1/2})U_{m-1}^k-[(\sigma_m^{k+1/2}+\sigma_{m-1}^{k+1/2})/2-1]\\&\times(G_{m-1}^{k+1/2}+G_m^{k+1/2})(U_m^{k+1/2}-U_{m-1}^{k+1/2}).\end{aligned}$$

If $|\sigma|>1$ we take the implicit scheme:

At the auxiliary level the formula is

$$(1+(\sigma^k_{m+1}+\sigma^k_m)/2)(G^k_m+G^k_{m+1})U^{k+1/2}_{m+1}+(1-(\sigma^k_{m+1}+\sigma^k_m)/2)(G^k_m+G^k_{m+1})U^{k+1/2}_m$$
$$=(G^k_m+G^k_{m+1})(U^k_{m+1}+U^k_m).$$

At the regular level the formula is

$$(1+(\sigma^{k+1/2}_{m+1}+\sigma^{k+1/2}_m)/2)(G^{k+1/2}_m+G^{k+1/2}_{m+1})U^{k+1}_{m+1}$$
$$+(1-(\sigma^{k+1/2}_{m+1}+\sigma^{k+1/2}_m)/2)(G^{k+1/2}_m+G^{k+1/2}_{m+1})U^{k+1}_m$$
$$=(G^{k+1/2}_m+G^{k+1/2}_{m+1})(U^k_m+U^k_{m+1})-(\sigma^{k+1/2}_m+\sigma^{k+1/2}_{m+1})$$
$$\times(G^{k+1/2}_m+G^{k+1/2}_{m+1})(U^k_{m+1}-U^k_m).$$

The above scheme is one-sided on boundaries. This lays a foundation for treating the values on the boundaries correctly.

3) Eliminate the unknown quantities at the inner points in the subregions by using the double sweep method. Then the unknown quantities on the boundaries can be obtained by using the discontinuity conditions and solving the equations with only the quantities on the boundaries.

4) Compute the unknown quantities at the inner points by using the difference equations and the quantities at the boundary points.

5) When the discontinuity lines interact with each other, use the subroutines for solving different sorts of Riemann problems to determine the velocities and the properties of the new discontinuity lines, and the initial values of the physical quantities in each new subregion. Then the coordinate transformation turns the new subregions into a strip on the ξ–t plane and the numerical computation will continue. The main subroutines are one for the Riemann solution in the non-reacting case and one for the Riemann solution with detonation and deflagration waves.

IV. Numerical Results

The ignition problem (including Example 1 (the same medium): $\gamma_0=\gamma_1=1.4$, $Q=20$, $\hat{Q}=2$, $K=0.1$; and Example 2 (different media): $\gamma_0=1.4$, $\gamma_1=1.35$, $Q=20$, $\hat{Q}=2$, $K=0.105$) and the accelerated flame problem (Example 3: $\gamma_0=\gamma_1=1.26$, $Q=27$, $\hat{Q}=2.6$, $K=0.03367$, $\Delta K=0.08667$) are computed. For the comparison the same data as in [2] are used in Examples 1 and 3 (only the data in Example 2 are different from [2]).

The distribution of the discontinuity lines in the case of Ex. 1 is given in Fig. 4. At $t=10.17$ the reflected shock wave interacts with the deflagration at the point $x=18.67$ and a C–J detonation appears. At $t=11.57$ another right-facing shock wave meets the C–J detonation at the point $x=29.01$ and a strong detonation forms. The distribution of the pressures at three different times in the case of Ex. 1 is given in Fig. 5,

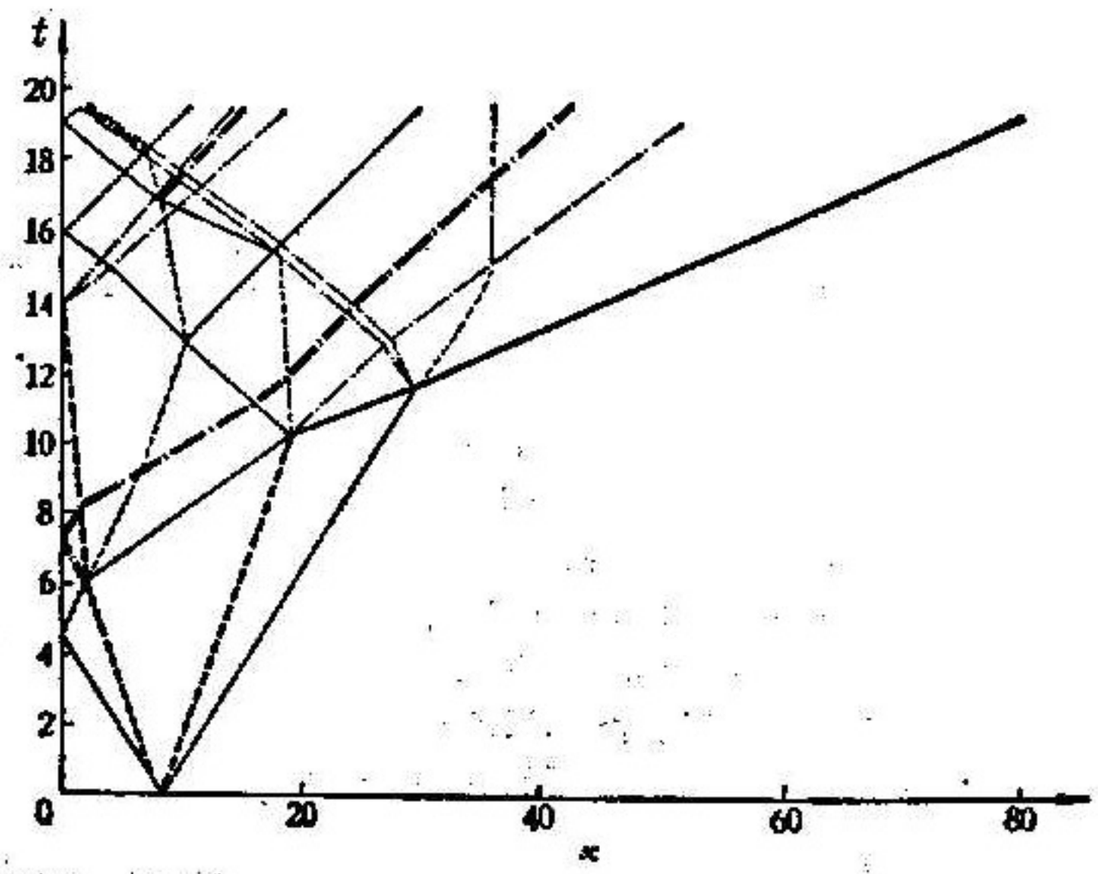

Fig. 4

——— contact dis., —·—·— rarefaction wave,
——— shock, - - - - - - - deflagration,
——— detonation, $\gamma_0=\gamma_1=1.4$ (Ex. 1).

where the difference of the pressures is seen to be the largest just at the time the deflagration becomes the C–J detonation. The distribution of the pressures in the case of Ex. 2 is given in Fig. 6. The results are similar to those in Ex. 1. The distribution of the discontinuity lines in the case of Ex. 3 is given in Fig. 7. At $t=64.93$ one contact discontinuity interacts with the deflagration at the point $x=61.22$ and the latter becomes a C–J detonation. Then at $t=66.44$ another contact discontinuity meets the C–J detonation and the latter becomes a strong detonation. The distribution of the pressures in the case of Ex. 3 is given in Fig. 8.

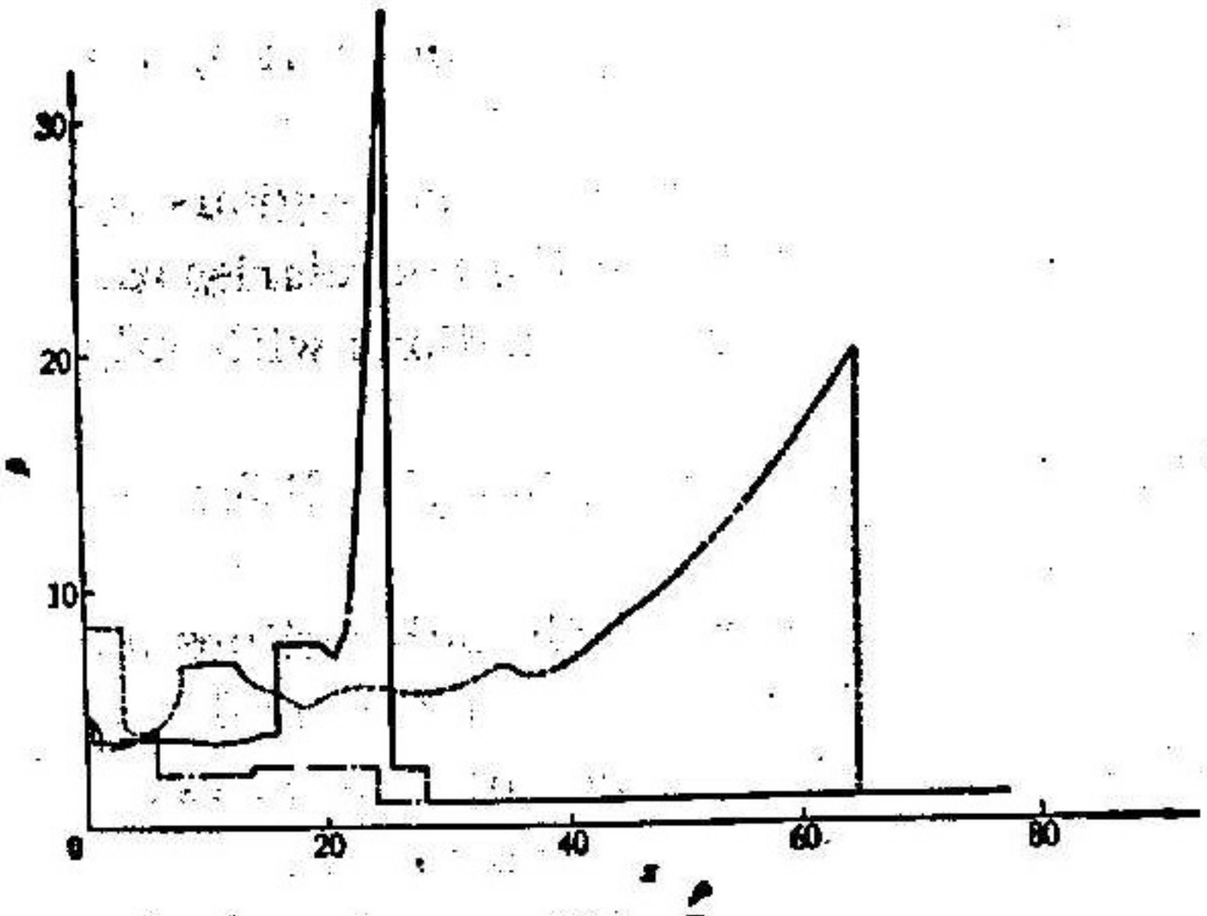

Fig. 5

—·—·— $t=9$, ——— $t=11$,
——— $t=17$, $\gamma_0=\gamma_1=1.4$ (Ex. 1).

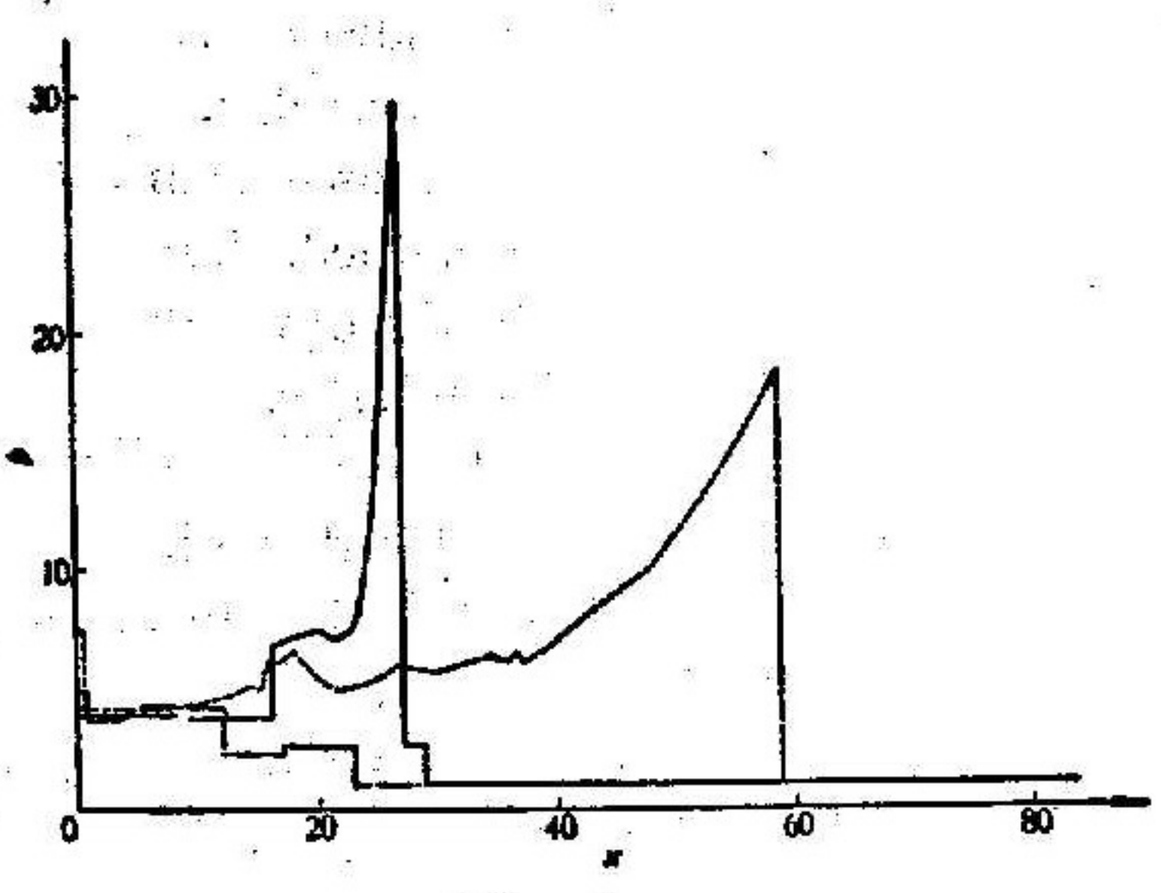

Fig. 6

—·—·— $t=9$, ——— $t=11$,
——— $t=17$, $\gamma_0=1.4$, $\gamma_1=1.35$ (Ex. 2).

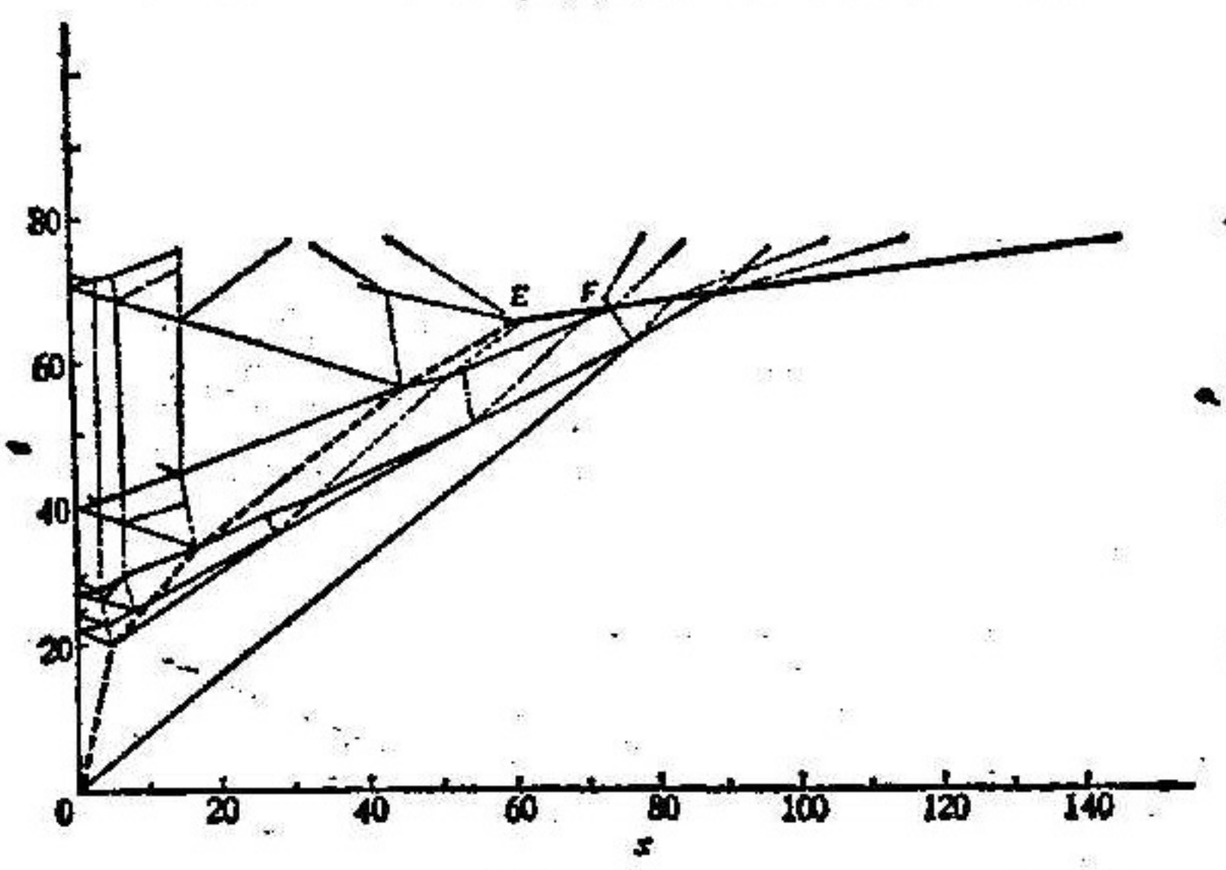

Fig. 7

——— contact dis.,
—·—·— rarefaction wave,
——— shock,
——— deflagration,
——— detonation.
E: $t=64.93$, $x=61.22$;
F: $t=66.44$, $x=72.24$ (Ex. 3).

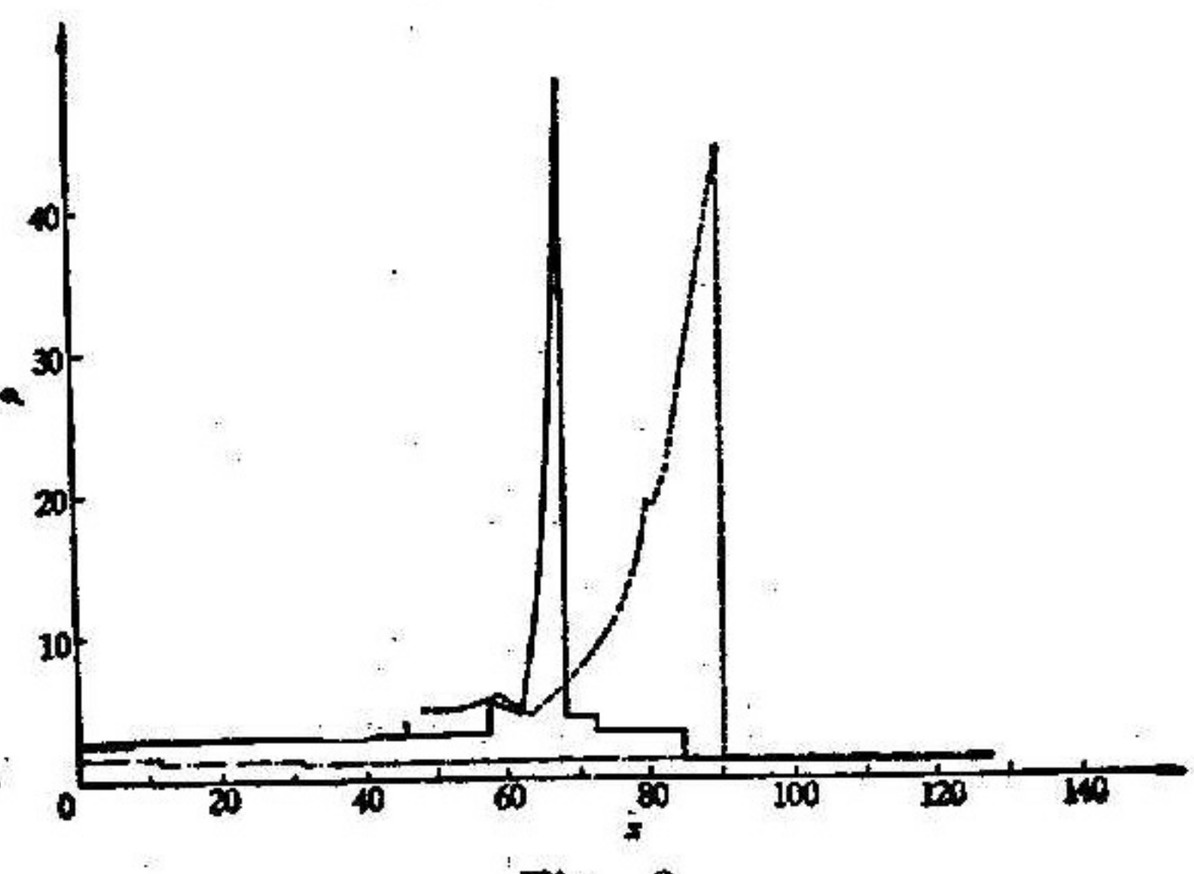

Fig. 8

—·—·— $t=25$,
——— $t=66$,
——— $t=69$.
(Ex. 3)

To test the correctness, accuracy and economic effectiveness of S. S. M., the following work has been done:

1) In S. S. M. two different sorts of meshes, that is, 4 mesh points and 7 mesh points in each subregion, are used. In the place near the combustion wave the

solutions have more than two significant digits. In other places the fractional error is about 1%—2% in a general way. (Some discontinuities with small strength are not separated.)

2) The distributions of the pressures at $t=8$ and $t=18$ in the case of Ex. 1 and at $t=40$ and $t=70$ in the case of Ex. 3, obtained from S. S. M. and from R. C. M., have been compared. The results are shown in Figs. 9—12. From the figures it is seen that R. C. M. is a method whose adaptability is very strong. For much more complicated problems basically correct physical figures without oscillation can be obtained by using R. C. M. Its results is basically in agreement with those from S. S. M. in respect of the structure of the figures. And for mildly complicated problems, when the space step Δx decreases from 1 to 0.5, the results of R. C. M. can be clearly seen to tend to those of S. S. M. (For instance, the results at $t=8$ in the case of Ex. 1 (Fig. 9) and those at $t=40$ in the case of Ex. 3 (Fig. 11) show this tendency.) But

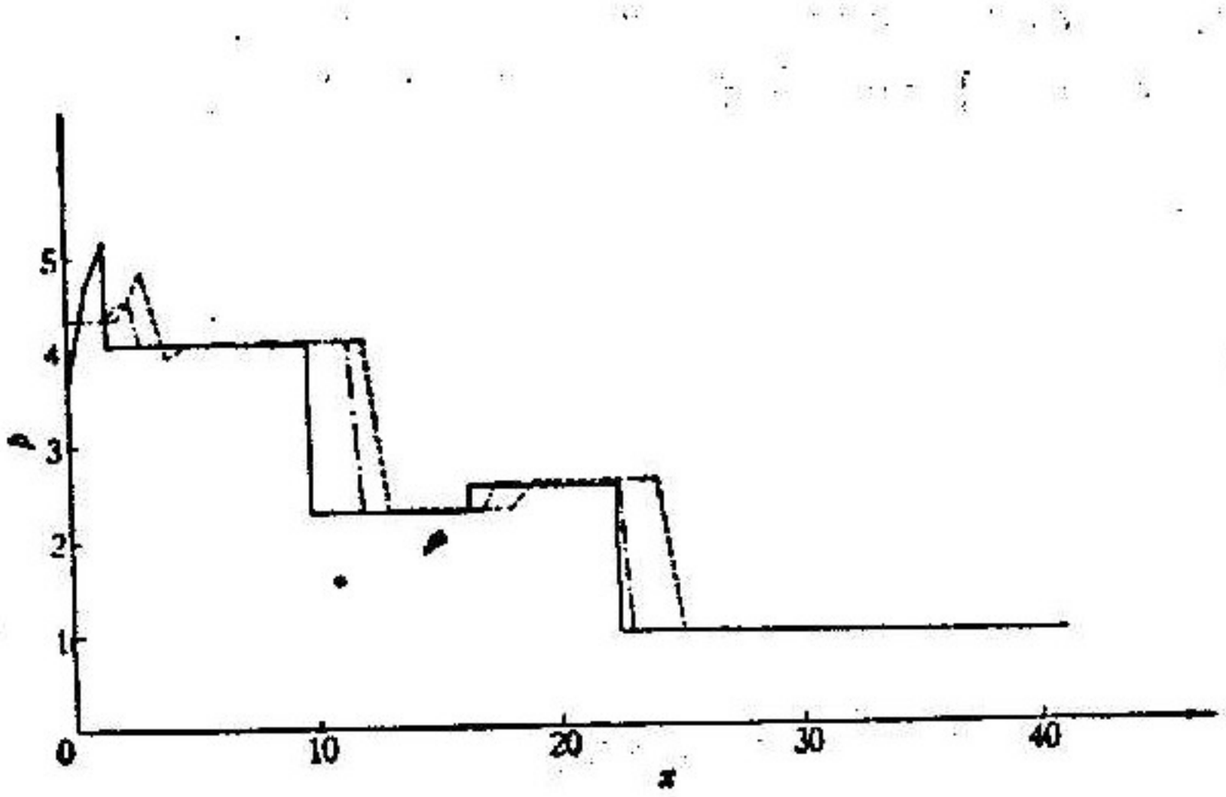

Fig. 9

——— S. S. M.,
——— R. C. M., $\Delta x=1$, group 1,
—·—·— R. C. M., $\Delta x=0.5$, group 1.
Ex. 1, $t=8$.

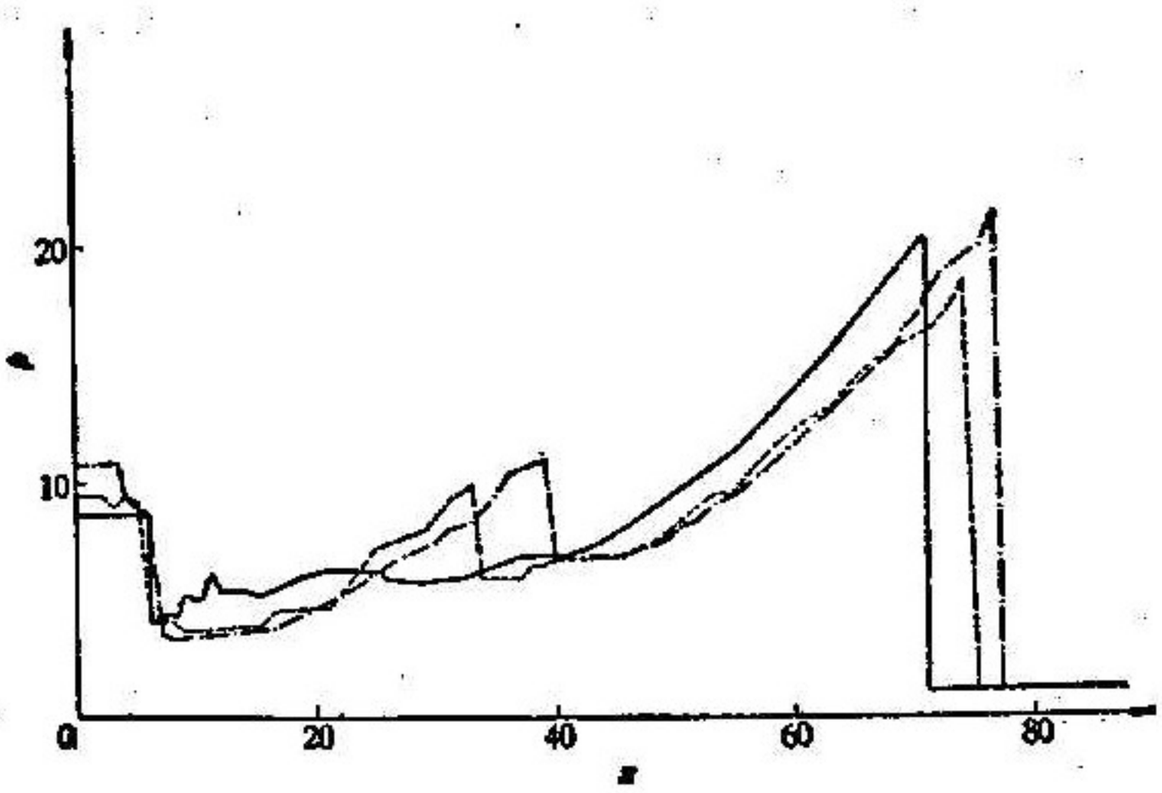

Fig. 10

——— S. S. M.,
——— R. C. M., $\Delta x=1$, group 1,
—·—·— R. C. M., $\Delta x=0.5$, group 1.
Ex. 1, $t=18$.

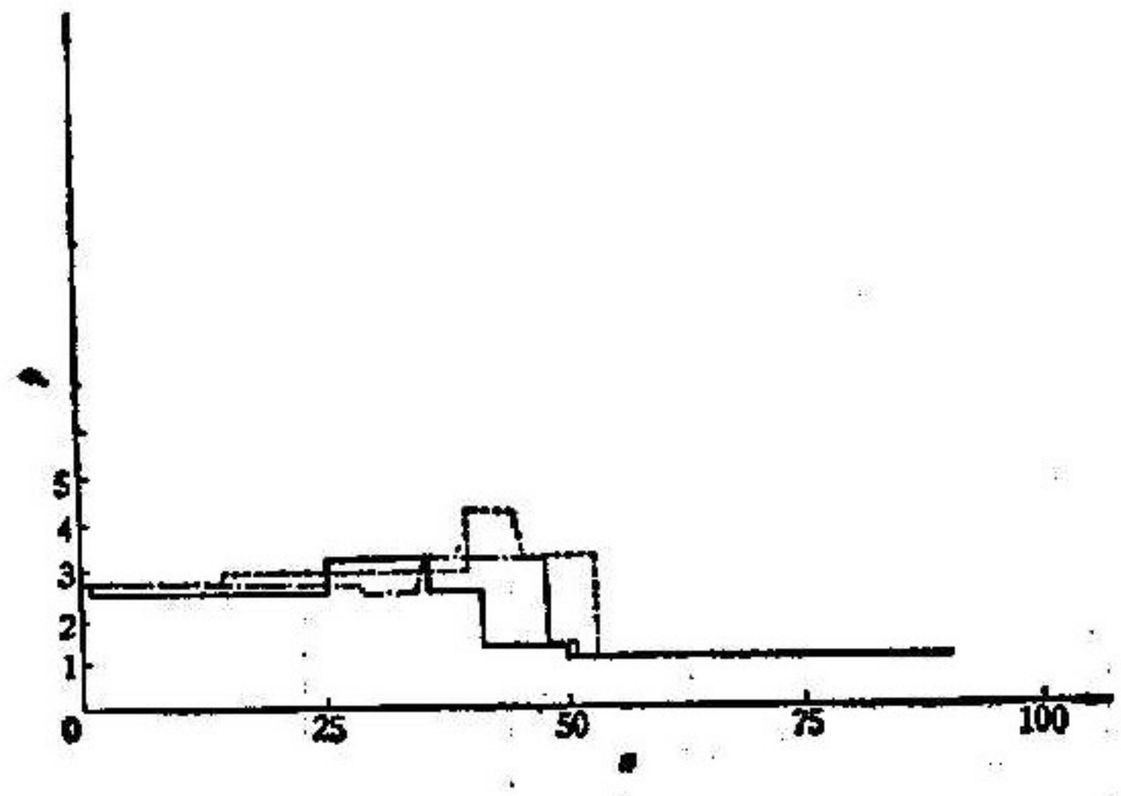

Fig. 11

——— S. S. M.,
——— R. C. M., $\Delta x=1$, group, 1,
—·—·— R. C. M., $\Delta x=0.5$, group 1.
Ex. 3, $t=40$.

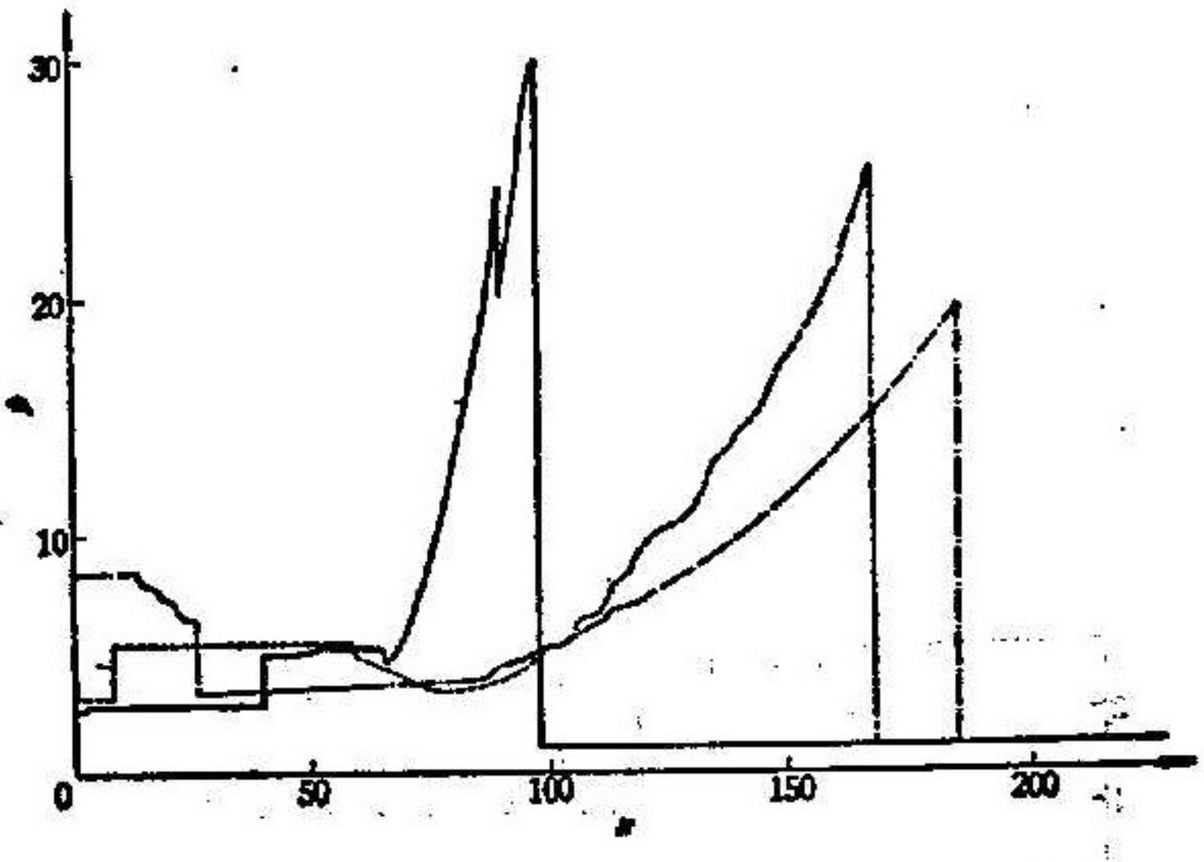

Fig. 12

——— S. S. M.,
——— R. C. M., $\Delta x=1$, group 1,
—·—·— R. C. M., $\Delta x=0.5$, group 1.
Ex. 3, $t=70$.

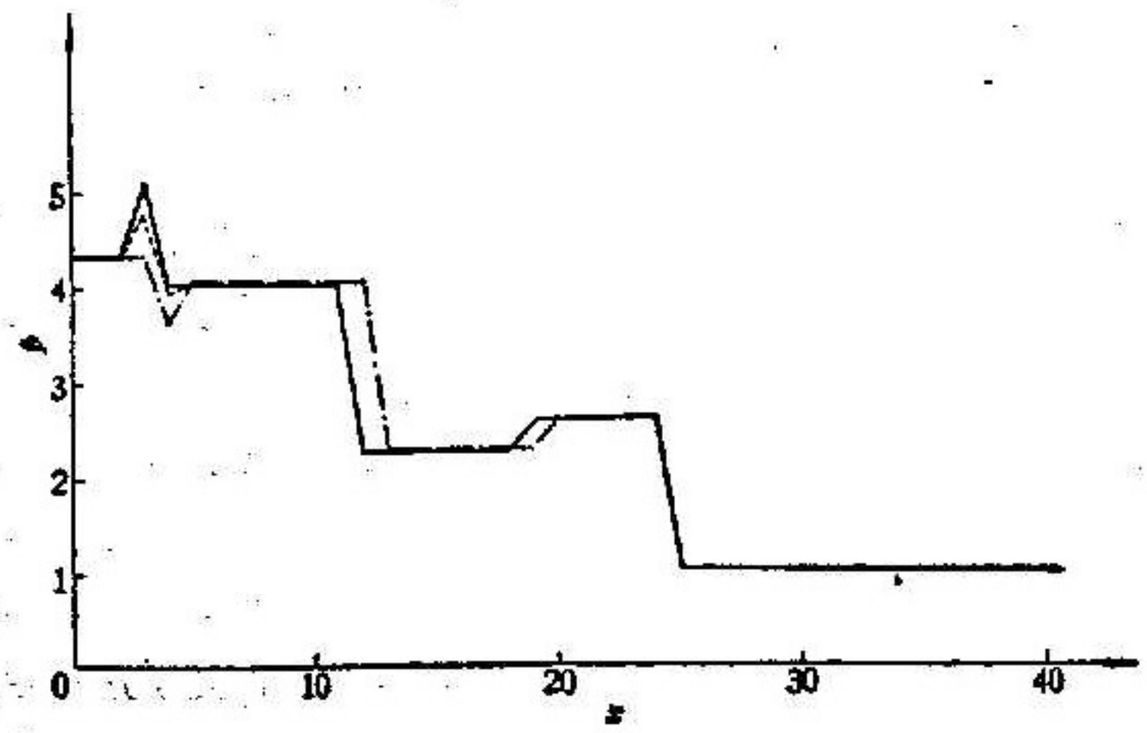

Fig. 13

——— group 1, ——— group 2,
— • — • group 3. Ex. 1 R. C. M., $\Delta x=1$, $t=8$.

the difference between the two results is still large from the point of view of quantitative analysis. For R. C. M. the results differ when different steps are used. To further investigate R. C. M., different random numbers are used. Figs. 13—17 show the results. From the figures it is seen that the choice of random numbers would influence remarkably the numerical results, and that the difference between the results obtained by different random numbers and the difference between the result of R. C. M. and that of S. S. M. are of the same order of magnitude. From the above analysis we think that the difference between the results is due to the errors of R. C. M.

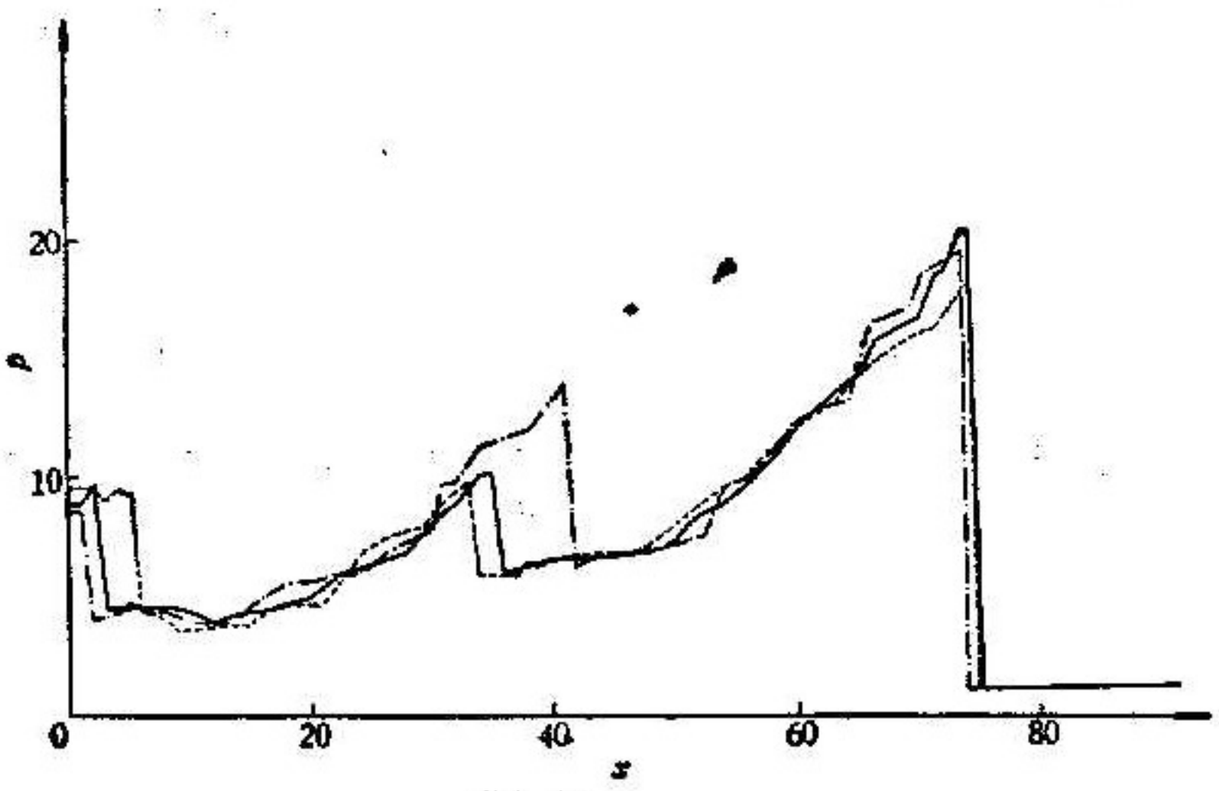

Fig. 14

——— group 1, —·—·— group 2,
——— group 3. Ex. 1 R. C. M., $\Delta x=1$, $t=18$.

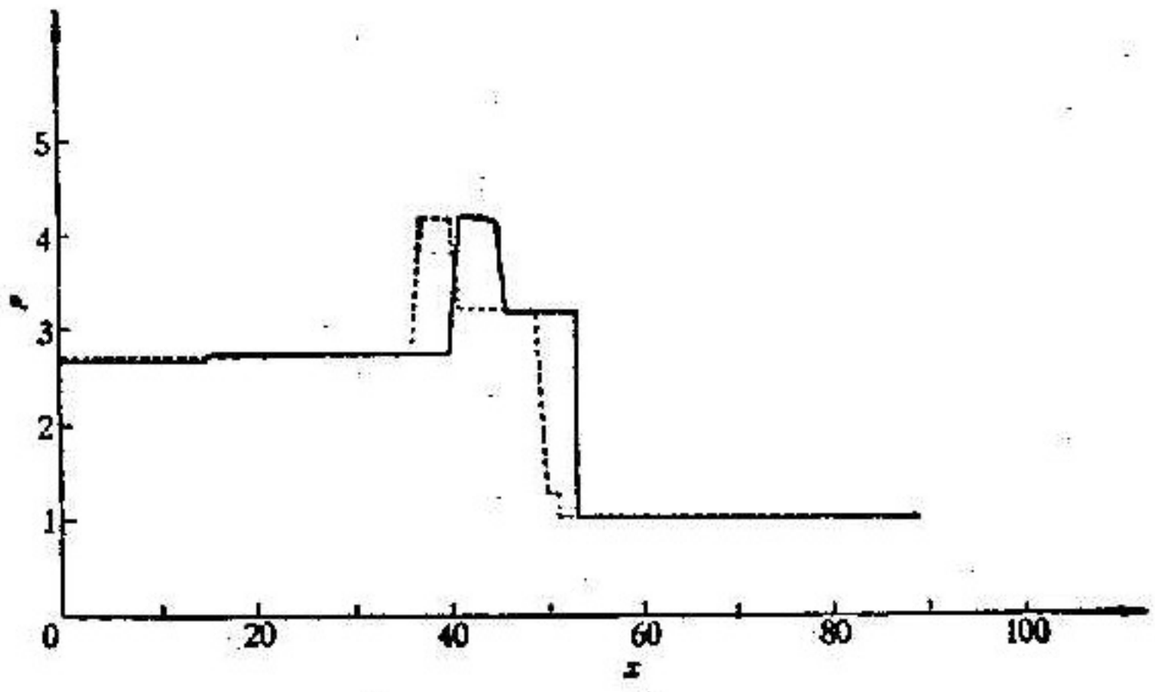

Fig. 15

——— group 1, ——— group 2.
Ex. 3 R. C. M., $\Delta x=1$, $t=40$.

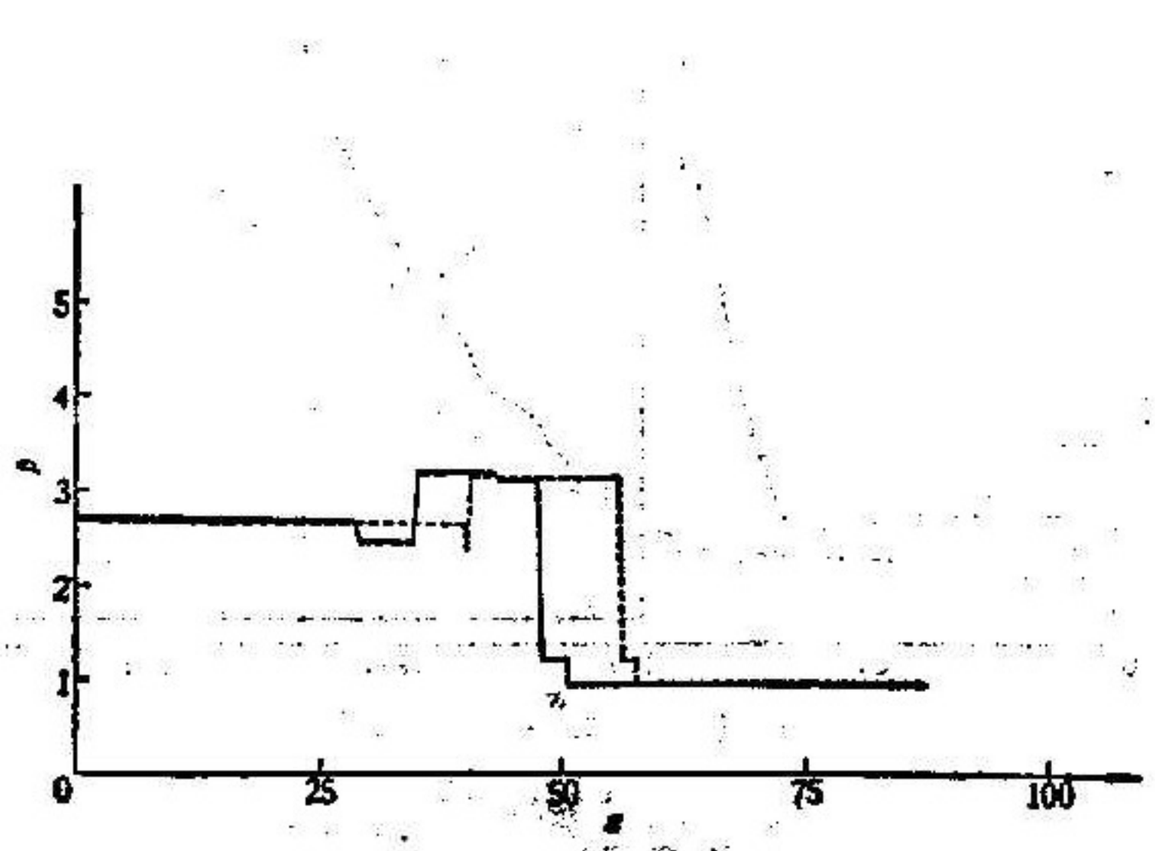

Fig. 16

——— group 1, ——— group 2.
Ex. 3 R. C. M., $\Delta x=0.5$, $t=40$.

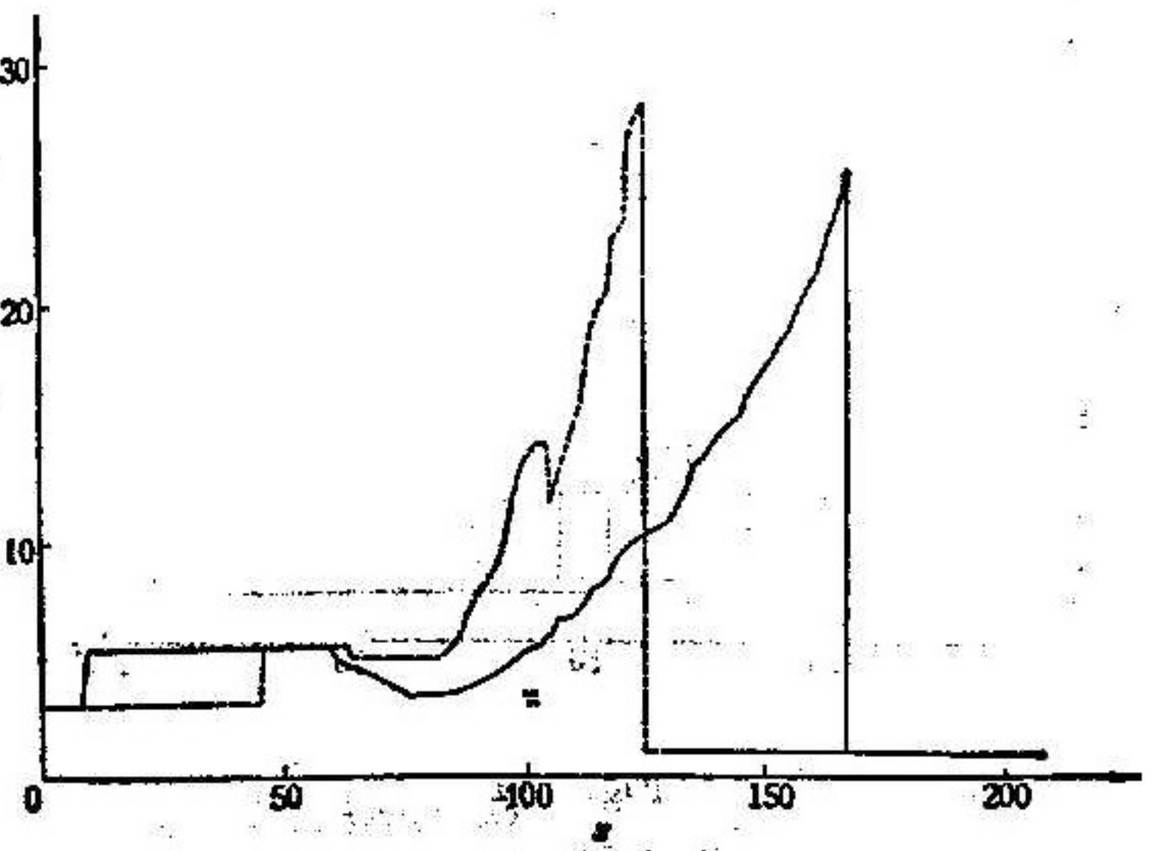

Fig. 17

——— group 1, ——— group 2.
Ex. 3 R. C. M., $\Delta x=1$, $t=70$.

3) We have compared the CPU time needed by the two methods. Table 1 shows the CPU time on IBM 4341 needed by the two methods for different computational grids. From the table it is known that R. C. M. needs much more time than S. S. M. because the Riemann problem must be solved at every mesh point in R. C. M.

Table 1 Comparison of CPU times

Ex.	Method	Number of mesh points or space step	Maximal number of mesh points in x direction	CPU time
Ex. 1 $t=0\sim20$	R. C. M.	$\Delta x=1$	88	2 minutes and 31 seconds (group 1*) 3 minutes and 1 seconds (group 2) 2 minutes and 44 seconds (group 3)
		$\Delta x=0.5$	178	14 minutes and 33 seconds (group 1)
	S. S. M.	4 points in each subregion	44	32.5 seconds
		7 points in each subregion	77	61 seconds
Ex. 2 $t=0\sim70$	R. C. M.	$\Delta x=1$	168	11 minutes and 20 seconds (group 1)
		$\Delta x=0.5$	370	60 minutes and 50 seconds (group 1)
	S. S. M.	4 points in each subregion	92	58.5 seconds
		7 points in each subregion	161	117 seconds

* Group 1 means the first group of random numbers.

The floating-shock-fitting method was used in [1] for the computation of a similar problem. Because the coordinate transformation in the x direction is used in S. S. M., the computational mesh is neater than that in [1]. Therefore, the adoption of this type of grid makes it easy to compute accurately very complicated physical problems such as the interactions of different discontinuities, and to show the physical figures at a certain time. Because only a little result is given in [1] we cannot give the comparison between our method and the method in [1] on accuracy, the CPU time and so on.

When S. S. M. is used in this problem, the number of the subregions is arbitrary. It depends on the structure of flow fields. The time step Δt can be shifted. At the time two discontinuity lines will soon interact, we change Δt and make the interaction of the two lines just at the next time step. In the computation we have used the techniques of dividing the intervals into several groups of intervals and the iteration method for solving the physical quantities on the boundaries. The details of these techniques can be found in [4].

References

[1] J. Kurylo, H. A. Dwyer, A. K. Oppenheim, Numerical analysis of flow fields generated by accelerated flames, *AIAA J.*, **18** (1980), 302—308.

[2] Zhen-huan Teng, A. J. Chorin, Tai-ping Liu, Riemann problems for reacting gas with applications to transition, *SIAM J. Appl. Math.*, **42** (1982), 964—981.

[3] A. J. Chorin, Random choice methods with application to reacting gas flow, *J. Comput. Phys.*, **25** (1977), 253—272.

[4] You-lan Zhu, Xi-chang Zhong, Bing-mu Chen, Zuo-min Zhang, Difference methods for initial-boundary value problems and flow around bodies, Science Press, Beijing, 1980.